Deactivation of a Cu/Al_2O_3 Catalyst in a N_2O Decomposition Reaction

Katsutoshi Tanaka, Atsushi Shimizu,*,† Masami Fujimori, Souhei Kodama, and Shigeki Sawai

Leona Plant, Asahi Kasei Corporation, Nagahama-cho, 4-3623, Nobeoka, Miyazaki 882-0854

†Performance Intermediates Business Development Dept., Asahi Kasei Corporation, Yuraku-cho, 1-4-2, Chiyoda-ku, Tokyo 100-8440

(Received July 29, 2002)

Dinitrogen oxide (nitrous oxide, N_2O), a non-CO_2 greenhouse gas, is produced as a by-product in the oxidation of cyclohexanone and cyclohexanol with nitric acid in adipic acid production plants. A Cu/Al_2O_3 catalyst has been used to decompose N_2O to nitrogen and oxygen. We investigated the rate of deactivation of Cu/Al_2O_3 to establish an industrial abatement process for N_2O. When Cu/Al_2O_3 catalyst containing 3 wt% of Cu was used, the apparent activation energy for the N_2O decomposition reaction was estimated to be 167 kJ mol^{-1} at 746–853 K and 113 kJ mol^{-1} at 853–953 K. The former activation energy has been ascribed to an inhibition effect of oxygen. The rate constants of the N_2O decomposition reaction have decreased with time. The decrease in the reaction-rates was analyzed by applying a first-order equation with respect to the rate constants. Simulation of the catalyst deactivation process has revealed that the Cu/Al_2O_3 catalyst is effective for at least for two years under the condition that 15 m^3 of the catalyst is used for an adipic acid plant with a production capacity of 120 kt per year. Thus, we have concluded that the catalyst is suitable for use in industrial processes.

Adipic acid is an important product in chemical industries because it is used as an ingredient of nylon 66, and also as an ingredient of aliphatic α,ω-dihydroxypolyester (so-called polyesterdiol), which is a soft segment of polyurethane. Dinitrogen oxide (nitrous oxide, N_2O), which is a non-CO_2 greenhouse gas, is generated in an almost stoichiometric amount during the production process of adipic acid, in which cyclohexanone or cyclohexanol is oxidized by nitric acid (Scheme 1). Thiemence and Trogler pointed out the significance of N_2O generated from adipic acid plants to the atmospheric N_2O budget.[1] It has been reported that the global generation of N_2O, which consists of both anthropogenic sources and natural sources, is estimated to be 26,000 kt per year.[2] The concentration of N_2O in the air is approximately 300 ppb at present. The amount of N_2O generation now exceeds the amount of N_2O decomposition globally, and is growing at a rate of 0.2% per year.[3,4] The amount of N_2O generation from adipic acid is reported to be 0.25 kg per 1 kg of adipic acid (survey by Miyazaki Prefecture in 1994). Therefore, the total amount of N_2O produced in adipic acid plants in the world is estimated to be ca. 580 kt/y in 1998 based on an adipic acid production of 2,300 kt/y (1 t = 10^3 kg). Because of the need to ensure conservation of the global environment, major adipic acid manufacturers have completed the introduction of N_2O abatement facilities to their adipic acid plants. Eighty percent of the N_2O generated at adipic acid plants around the world is now decomposed before it is released to the environment.[5]

Industrial N_2O abatement technologies consist mainly of a catalytic decomposition method and a thermal decomposition method.[5–8] Li and Armor have reported that many metals, such as Cu, Co, Ni, Mn, Fe, Rh, Ru, Pd, and Pt, exhibit decomposition activity.[9] A review of the subject has also been published recently.[10] The deactivation of catalysts as well as their catalytic activity is of great concern in industrial N_2O abatement processes, though few studies have examined this point.[8,11] Catalyst deactivation is generally ascribed to inhibition, poisoning, pore blocking, carbon deposition, sintering, phase transition, physical damage and the like. The design of a catalytic process is affected by these deactivation mechanisms. An estimation of the expected lifetime of a catalyst is also important in terms of the process design and process operation. The high levels of activity of copper catalysts are quite interesting from the viewpoint of practical applications, since copper catalysts have approximately the same activities as noble metals.[9] Our aim in this study is to examine the catalytic activity and the lifetime of Cu/Al_2O_3 under a high O_2 concentration and to in-

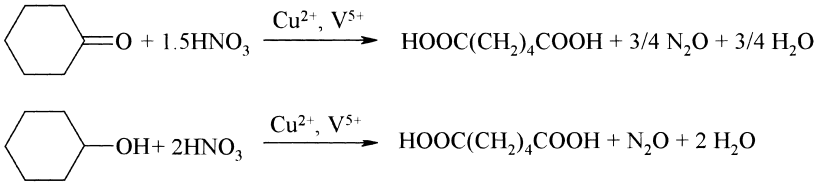

Scheme 1. Nitric acid oxidation of cyclohexanone and cyclohexanol.

Table 1. Decomposition Conditions of Dinitrogen Oxide

	Cat. weight	Cat. vol	Cat. hight	Cu	SV/10,000	N_2O feed	O_2 feed	θ at 298 K	Temp	N_2O Conv.
	g	mL	mm	wt%	h^{-1}	vol%	vol%	s	K	%
Run 1	3.00	3.5	10	2.96	0.964–3.28	13.1–32.6	18.2–14.2	0.110–0.458	746–916	4.30–89.9
Run 2	2.00	1.8	5	2.96	1.04–4.34	32.6–34.5	5.50–12.6	0.0830–0.345	773–953	7.00–60.1
Run 3	3.75	4.8	13.5	0.80	3.3	13.1	18.2	0.109	821–865	5.50–14.0
Run 4	3.75	4.4	12.5	2.40	3.56	13.1	18.2	0.101	770–858	1.31–24.9
Run 5	3.75	4.6	13	3.99	3.42	13.1	18.2	0.105	770–863	4.32–34.8
Run 6	7.50	10.6	32	0.00	1.44	13.1	18.2	0.250	873	12.1–12.8

θ: Reaction time. N_2O was used from a cylinder in Run 1 and Run 3–6. Take-off gas from adipic acid plant was used in Run 2. Air was used as dilution gas.

vestigate the possibility of industrial applications of Cu/Al_2O_3 to an N_2O abatement process.

Experimental

Preparation of Catalysts. Cu/Al_2O_3 catalysts were prepared by drying γ-Al_2O_3 impregnated with an aqueous solution of copper(II) nitrate, and then baking it at 773 K for 3 hours. The gamma- Al_2O_3 used in this study was a spherical activated alumina RN (material, γ-Al_2O_3 made from baked boehmite; size, 6–12 mesh; Al_2O_3, 99.7%; SiO_2, 0.1%; pore volume, 0.47 mL g^{-1}; average diameter of pore, 5.2 nm) manufactured by Mizusawa-Kagaku.

Measurement of Initial Activities. The catalysts were inserted into a tubular reactor (length, 500 mm; external diameter, 27.2 mm; internal diameter, 21.6 mm; material, 304 stainless steel) which was then introduced into an electric furnace. The temperature was controlled automatically by feedback of the temperature at the catalyst bed. A thermocouple, which was movable along the major axis of the reactor, was inserted into the reactor in order to measure the reaction temperatures. The feed-gas was a mixture introduced from a dinitrogen oxide cylinder and an air cylinder. The concentration of N_2O was 10–35%. The gas stream flowed in an upward direction, and the rate of gas flow was measured using a flowmeter. Dinitrogen oxide was decomposed at atmospheric pressure. The concentrations of the gaseous components were measured by gas chromatography (stainless steel column 3 mm $\phi \times 3$ m; Porapack Q for CO_2 and N_2O analysis; Molecular sieves 5A for N_2 and O_2 analysis; flow rate of He, 30–40 mL min^{-1}; column temp., 40–60 °C). The reaction temperatures were obtained by averaging the temperatures at the inlet, the center, and the outlet of the catalyst bed.

Measurement of Catalyst Deactivation. The deactivation of the catalysts was measured using the same instrument as that used for measuring the activities of the catalysts. Dinitrogen oxide was generated in the reactor of an actual adipic acid plant via a mist separator. The feed-gas was prepared by mixing dinitrogen oxide and air. The typical concentrations of N_2O, N_2, O_2, and CO_2 in the take-off gas from the adipic acid plant were 51 mol%, 40 mol%, 4 mol% and 5 mol%, respectively. Water vapor was at the saturated vapor pressure.

Results and Discussion

Initial Activities of Catalysts. N_2O was decomposed under the conditions listed in Table 1. The apparent rate constants, k_a s^{-1}, were obtained by measuring the concentrations of N_2O at the outlet of the reactor at various temperatures. The reaction was treated as a first-order reaction assuming a plug flow. The following equations were used:

$$r_{N_2O} = k_a \cdot (P_{NO_2}/RT), \quad (1)$$

$$k_a\theta = -(1 + \varepsilon) \ln (1 - X) - \varepsilon X, \quad (2)$$

where k_a, P_{NO_2}, R, T, θ, ε, and X denote the apparent rate constant, partial pressure of N_2O, gas constant, temperature, reaction time, variation of gas volume due to the reaction, and the extent of the reaction, respectively. Figure 1 shows Arrhenius plots. When the concentration of Cu in the catalyst was 3.00 wt%, the apparent activation energies were estimated to be 167 kJ/mol at 746–853 (Line B in Fig. 1) and 113 kJ mol^{-1} at 853–953 K (Line A in Fig. 1) from Runs 1 and 2. The value reported in the literature, 135 kJ mol^{-1} ($Cu(4.9\ wt\%)/Al_2O_3$), is between those values.[12] The supporting matrix of Al_2O_3, itself, had a low decomposition activity (Run 6 in Fig. 1), and the reaction rate increased with the Cu concentration, but reached a ceiling at around 4 wt% of Cu concentration (Fig. 2). In investigating the deactivation of the catalyst, we determined the concentration to be 3%. N_2O from a cylinder was used in Run 1, but N_2O from an actual adipic acid plant was used in Run 2. Water was included in the ingredients in Run 2. Although water can inhibit a decomposition reaction of N_2O,[10] the inhibiting effect on the reaction need not be taken into account in this experiment, since the Run 1 and 2 reaction rates were consistent with each other.

Deactivation of the Catalyst. We examined the deactivation of the catalyst under the conditions given in Table 2, using actual take-off gas from an adipic acid plant and Cu/Al_2O_3 onto which 3.0% of Cu had been adsorbed. The N_2O loads

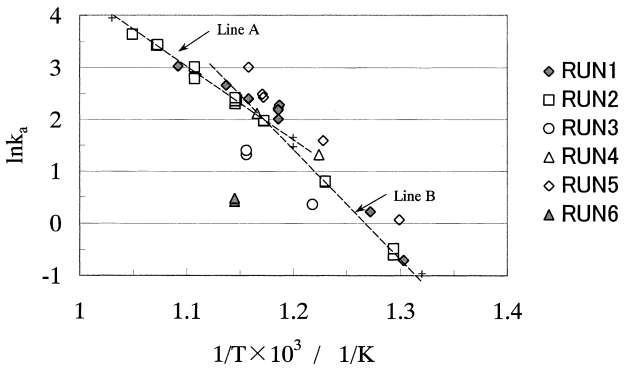

Fig. 1. Arrhenius plots for N_2O decomposition.
746–853 K $\ln k_a = 25.76 - 20242/T$ (Line B).
853–953 K $\ln k_a = 17.88 - 13523/T$ (Line A).

Table 2. Conditions for Evaluating the Deactivation of Cu/Al_2O_3

	Cat. weight	Cat. hight	Gas feed	LV (NPT)	SV (NPT) /10,000	N_2O	N_2O conc.	O_2 conc.	CO_2 conc.	Max temp	Av temp	N_2O conv.
	g	mm	NL h^{-1}	h^{-1}	h^{-1}	kmol m^{-3} h^{-1}	mol%	mol%	mol%	K	K	%
Run 7	7.5	30	76.5	6.40	0.77	110	33.2	4.9	3.2	685	664	91–77
Run 8	7.5	30	35.0	2.90	3.52	50	34.3	4.2	3.4	685	676	92–91
Run 9	4.0	16	76.5	6.40	1.44	206	32.7	5.7	3.2	685	668	84–74
Run 10	7.5	29	153	12.8	1.59	110	16.4	12.3	1.7	685	667	87–76
Run 11	7.5	29	153	12.8	1.59	55	8.2	16.7	0.8	685	674	94–90
Run 12	7.5	29	153	12.8	1.59	55	8.0	16.9	0.8	600	594	55–46
Run 13	7.5	25	153	12.8	1.743	54	8.0	16.9	0.8	530	528	11

In Run 8, the catalyst which was used in Run 7 was evaluated.

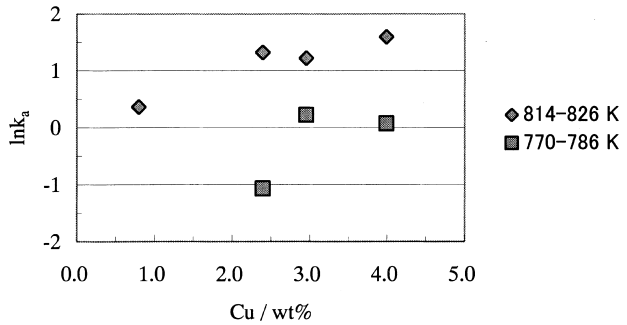

Fig. 2. Cu weight dependence of N_2O decomposition rate constants.

were higher than the assumed values for the process in order to accelerate the deactivation. As shown in Fig. 3, $\log k_a$ decreased linearly with time. Catalyst deactivation is generally explained as a function of the concentration of inhibitors and the rate constant, as follows:[13]

$$-\frac{dq}{dt} = \alpha q^n C_i^m, \quad (3)$$

where q is the rate constant, α is the deactivation rate constant, and C_i is the concentration of inhibitor. As described earlier, the inhibition effect of water was negligible in this experiment, and $\log k_a$ decreased almost linearly with time (Fig. 3). Thus, the rate equation of the deactivation is simplified as follows:

Table 3. Deactivation Rate Constants α for Cu/Al_2O_3

	Run 7	Run 8	Run 9	Run 10	Run 11	Run 12
α day^{-1}	0.032	0.005	0.023	0.04	0.017	0.012
Av temp/K	937	949	941	940	947	867

$$-\frac{dk_a}{dt} = \alpha k_a. \quad (4)$$

Table 3 summarizes the deactivation rate constants (α) which are obtained from the slopes of the lines in Fig. 3. These deactivation rate constants (α) are not solely dependent on the temperatures. As shown in Fig. 4, α seems to be related to the amount of N_2O that has reacted. The decomposition reaction of N_2O is exothermic, and its heat of reaction is 82.0 kJ mol^{-1}. This relatively large amount of heat of reaction probably accelerates the deactivation around the active site on the catalyst surface. Copper-based catalysts are more susceptible to temperature than other commonly used metallic catalysts.[14] The specific surface area of the catalyst was 145 m^2/g before the experiment, which decreased to 115 m^2/g after the experiment. These facts suggest that the thermal sintering of Cu or alumina are possible mechanisms of deactivation.

Influence of Oxygen on the Dinitrogen Oxide Decomposition Reaction. Figure 1 indicates that the activation energy of the decomposition reaction at lower temperatures (746–853 K) is larger than that at higher temperatures (853–953 K). This is probably because the inhibiting effect of oxygen increases at

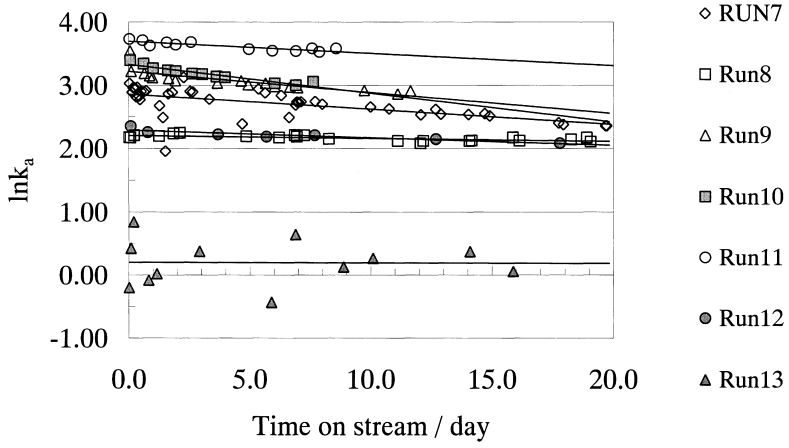

Fig. 3. Variations in rate constants of N_2O decomposition with Cu/Al_2O_3.

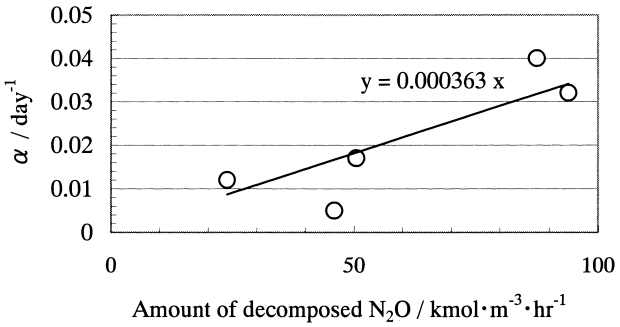

Fig. 4. Relationship between the deactivation constants α and the amount of reacted N_2O.

the lower temperature. As for the reaction mechanism, Rheaume and Parravano have explained that N_2O is first adsorbed onto the catalyst (Eq. 5), where it is converted to a nitrogen molecule and an oxygen atom (Eq. 6), and then the oxygen is eliminated from the surface of the catalyst (Eq. 7),[15] as shown by the following equations:

$$N_2O + * \underset{k_{-1}}{\overset{k_1}{\rightleftharpoons}} N_2O^* \quad K_{N_2O} = k_1/k_{-1}, \tag{5}$$

$$N_2O^* \xrightarrow{k} N_2 + O^*, \tag{6}$$

$$2O^* \underset{k_2}{\overset{k_{-2}}{\rightleftharpoons}} O_2 + 2* \quad K_{O_2} = k_2/k_{-2}, \tag{7}$$

where $*$, N_2O^* and O^* denote the active site, the adsorbed dinitrogen oxide and the adsorbed oxygen atom, respectively. The influence of mass transfer for a laminar film should not be important in this study because the rate constants were not dependent on the space velocity (SV) in Run 1 and Run 2. Therefore, the reaction rate due to mass transfer is not included in the following discussion. If Eq. 6 is a rate-determining step and the N_2O^* and O^* that are adsorbed on the catalyst are in stationary states, the rate of reaction r_{N_2O} can be represented by the Langmuir–Hinshelwood equation,

$$r_{N_2O} = \frac{kN_TK_{N_2O}(P_{N_2O}/RT)}{1 + K_{N_2O}P_{N_2O} + K_{O_2}^{1/2}P_{O_2}^{1/2}}, \tag{8}$$

where N_T (mol L^{-1}) denotes the number of active sites on the surface of the catalyst.[16] The Langmuir-Hinshelwood equation is introduced when

$$-[O^*]^2 + K_2P_{O_2}[*]^2 = 0 \tag{9}$$

is presumed, which is a modified form of Eq. 10 with the condition that its first component is negligible ($k \ll k_{-2}$). The following equation explains the approximation for the stationary state of oxygen adsorbed on the surface of the catalyst:

$$\frac{k}{k_{-2}}[N_2O^*] - [O^*]^2 + K_{O_2}P_{O_2}[*]^2 = 0. \tag{10}$$

Dandekar and Vannice have reported that Eqs. 6 and 7 are rate-determining steps and K_{N_2O} is 0.26–0.05 atm^{-1} at 473–573 K.[12] If these data are extrapolated to the temperature of our study, K_{N_2O} is calculated to be less than 0.001 at above ca. 620 K, which is sufficiently small. If K_{N_2O} is sufficiently smaller than K_{O_2} ($K_{N_2O} \ll K_{O_2}$) and the O_2 concentration is sufficiently large, then $[N_2O^*]$ is sufficiently smaller than $[O^*]$ ($[N_2O^*] \ll [O^*]$). Therefore, the first component of Eq. 10 can be considered to be negligible compared to the second, even if k is roughly equal to k_{-2}. Eventually, Eq. 8 should be applicable based on the condition of high O_2 concentration, such as in this experiment, whether or not Eq. 7 (k_{-2}) is the rate-determining step. If $K_{N_2O}P_{N_2O}$ is sufficiently small compared to 1, the reaction rate can be explained as follows:

$$r_{N_2O} = kN_TK_{N_2O}\frac{1}{1 + K_{O_2}^{1/2}P_{O_2}^{1/2}}(P_{N_2O}/RT). \tag{11}$$

Thus, k_a of Eq. 1 is represented by

$$k_a = kN_TK_{N_2O}\frac{1}{1 + K_{O_2}^{1/2}P_{O_2}^{1/2}} = kN_TK_{N_2O}f, \tag{12}$$

$$f = \frac{1}{1 + K_{O_2}^{1/2}P_{O_2}^{1/2}}. \tag{13}$$

If the inhibiting effect (f) of oxygen is negligible at higher temperatures, f at lower temperatures (746–853 K) can be derived from the difference between two Arrhenius plots, which are Line A and Line B in Fig. 1, and then K_{O_2} can be calculated from f. Those results are indicated in Table 4 and Fig. 5. The adsorption equilibrium constants (K_{O_2}) calculated from the above procedures show good linearity with $1/T$. These values of f, followed by K_{O_2}, were used to simulate the simulation of the catalyst deactivation described below.

Table 4. Adsorption Equilibrium Constants for O_2 on Cu/Al_2O_3

Temp	$\ln k_a$		P_{O_2}	K_{O_2}
K	Experimental	Corrected	atm	atm^{-1}
746	−1.21	−1.36	0.149	28.9
767	−0.71	−0.62	0.151	13.0
786	0.22	0.01	0.157	5.7
813	0.81	0.86	0.078	2.8

Corrected values are calucalated from. $\ln k_a = 25.76 - 20242/T$ (Line B in Fig. 2).

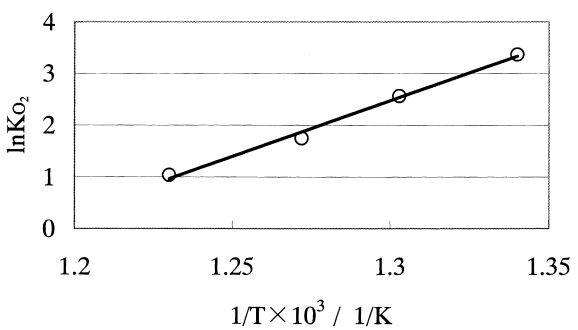

Fig. 5. Temperature dependence of the adsorption equilibrium constants of O_2 on Cu/Al_2O_3, $\ln K_{O_2} = 21513 \cdot 1/T - 25.495$.

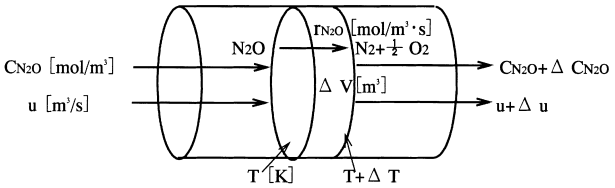

Fig. 6. Mass balance and heat balance of the plug flow reactor.

Simulation of the Catalyst Deactivation. The purpose of the simulation was to calculate the changes in the reaction temperatures, the flow rates of N_2O, the decomposition rates of N_2O and the relative activities along the axis of the N_2O decomposition reactor with respect to time. The equations for the mass balance and the heat balance in the simulation were introduced by the following procedures. We assumed an adiabatic tubular reactor that used a plug flow system (Fig. 6). Taking into account the expansion of the gas volume due to the increase in temperature and the increase in the number of moles, the mass balance at volume element ΔV (m^3) of a plug flow reactor can be represented by Eq. 14, as follows:

$$\Delta V \cdot r_{N_2O} + u \cdot C_{N_2O} - (u + \Delta u) \cdot (C_{N_2O} + \Delta C_{N_2O}) = 0, \quad (14)$$

where r_{N_2O} (mol m^{-3} s^{-1}) denotes the reaction rate, u (m^3 s^{-1}) denotes the flow rate of gas, Δu (m^3 s^{-1}) denotes the difference in the flow rate of gas before and after the volume element, C_{N_2O} (mol m^{-3}) denotes the concentration of the reactant, and ΔC_{N_2O} (mol m^{-3}) denotes the difference in the concentration of the reactant before and after the volume element. When the catalyst is placed in a cylindrical reactor with a (m) of diameter, Eq. 15 is obtained from Eq. 14 using the differential form with the reactor length L (m),

$$\pi a^2 r_{N_2O} - u \frac{dC_{N_2O}}{dL} - C_{N_2O} \frac{du}{dL} = 0. \quad (15)$$

The heat balance at volume element ΔV (m^3) is represented by

$$\Delta V \cdot r_{N_2O} \cdot \frac{\Delta H}{C_p \cdot n} = \Delta T, \quad (16)$$

where ΔH (kJ mol^{-1}) denotes the heat of reaction, C_p (kJ K^{-1} mol^{-1}) the specific heat at constant pressure, n (mol s^{-1}) the total flow rate of gases and ΔT (K) the difference in the temperature before and after the volume element. The following equation follows from Eq. 16 using the differential form with the reactor length L (m):

$$r_{N_2O} \pi a^2 \Delta H \cdot \frac{1}{C_p} \frac{1}{n} - \frac{dT}{dL} = 0. \quad (17)$$

A simulation was executed using the integration of those two equations (Eq. 15 and Eq. 17). The Ruhge–Kutta method was used for the integration. The reaction rate (r_{N_2O}) in Eqs. 15 and 17 was calculated by using Eq. 11. The inhibiting effect (f) of oxygen to the N_2O decomposition reaction in Eq. 11 was calculated using the temperature dependence of ln K_{O_2} shown in Fig. 5. An activation energy of 113 kJ mol^{-1}, which was the value at over 853 K, was used to calculate k in Eq. 11. The decrease in k with time in Eq. 11 was calculated by Eq. 4, and the deactivation rate constant (α) was obtained from Fig. 4 (α day^{-1}) = 3.63 × 10^{-4} × (the amount of N_2O reacted [kmol m^{-3} h^{-1}])). The production capacity of the adipic acid plant was assumed to be 120 kt y^{-1}. The concentration of N_2O from the nitric acid oxidation in an adipic acid plant was about 50%. If N_2O is treated without dilution, the reaction temperature would rise too much, such that NO_x would be generated. Therefore, dilution of N_2O to 10% concentration was presumed. Table 5 summarizes the initial condition for the calculation. The hypotheses for the simulation, which have been mentioned already, are listed again below:

(1) $K_{NO_2} \ll K_{O_2}$ on Cu/Al_2O_3.

(2) The N_2O decomposition reaction is inhibited by O_2 at below 853 K.

(3) The decreasing rate of the apparent decomposition reaction rate of N_2O (k_a) has a first-order dependency with respect to k_a.

(4) The deactivation rate constant (α) of k_a is mainly related to the amount of N_2O reacted.

Based on these hypotheses, the results of a simulation of the reaction temperatures, the flow rates of N_2O, the decomposition rates of N_2O and the relative activities with the length of the reactor are described below.

Figure 7a shows the calculated profile of the temperatures. The point where the maximum temperature is reached moves toward the exit of the reactor in accordance with the progress of catalyst deactivation. Fig. 7b shows the calculated results for the remaining N_2O flow rate in the reactor. This curve shows that 15 m^3 of the catalyst lasts 600 days. The availability of this amount of catalyst is feasible in an actual plant. As

Table 5. Conditions for the Simulation of Catalyst Deactivation

Production capacity of adipic acid		120 kt y^{-1}
Rate of N_2O generation		0.25 t/t-adipic acid
The number of days worked of the plant in a year		300 days
Take-off gas from adipic acid plant	N_2O	26.3 mol s^{-1}
	N_2	23.2 mol s^{-1}
	O_2	2.06 mol $s-^{1}$
Air for dilution		211 mol s^{-1}
Reactor diameter		3.60 mϕ
Temperature at inlet		773 K
Pressure at inlet		2.10 atm
Heat of reaction		82.0 kJ mol^{-1}
Heat capacity at constant pressure		32.0 J K^{-1} mol^{-1}

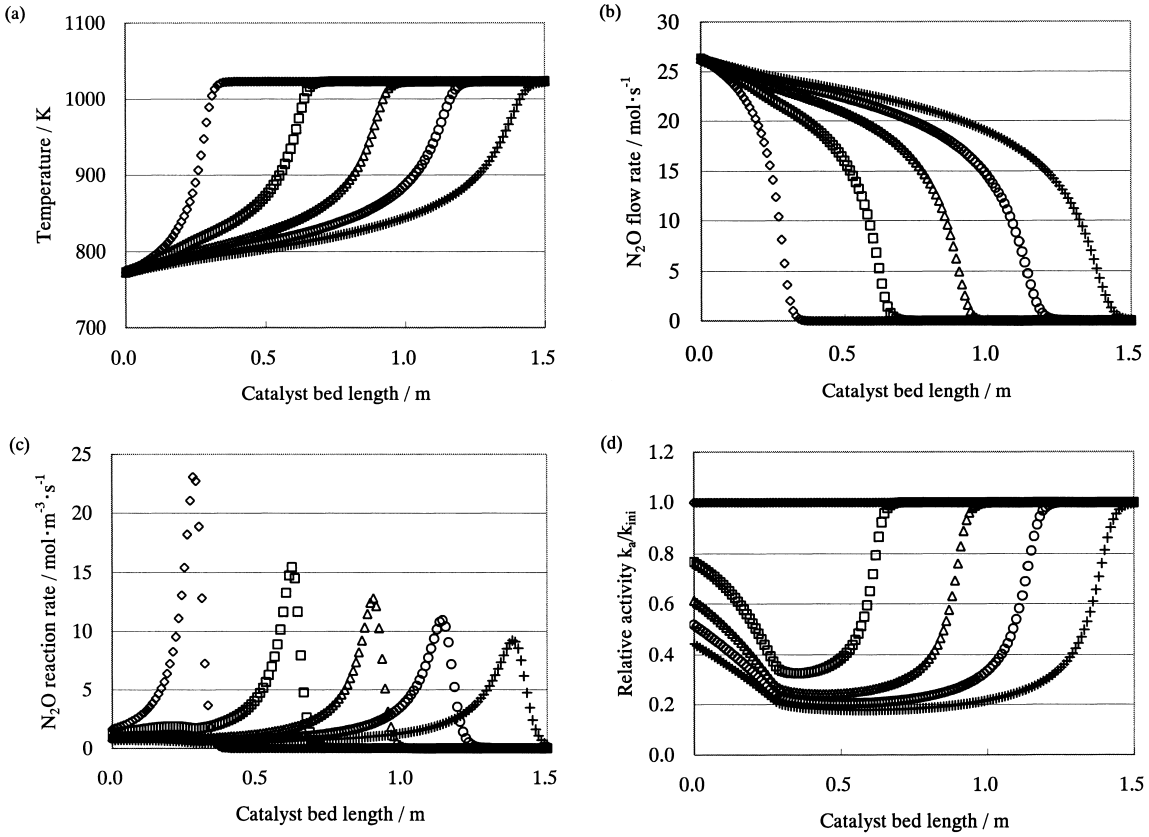

Fig. 7. Simulation results of N_2O decomposition reaction with Cu/Al2O_3. (a) Simulation of the reaction temperatures. (b) Simulation of the flow rates of N_2O. (c) Simulation of the decomposition rates of N_2O. (d) Simulation on the relative activities ◇: initial, □: 150 days, △: 300 days, ○: 450 days, +: 600 days.

shown in Fig. 7c, the point that shows the maximum rate of N_2O decomposition moves toward the exit of the reactor in accordance with the progress of catalyst deactivation. The point where the decomposition rate is at a maximum is the point where the rate of deactivation is at maximum. The relative activity (k_a/k_{ini}), which is the ratio of the rate constant of the spent catalyst to the rate constant of a fresh catalyst, indicates the degree of deactivation (Fig. 7d). The deactivation of the catalyst begins from the inside of the catalyst bed and progresses through the whole reactor. Eventually, the catalyst is deactivated to an almost equal degree throughout the catalyst bed.

The increase in temperature during the decomposition process of N_2O is large, since the concentration of N_2O from an adipic acid plant is large. If we use the heat of reaction to preheat the feed-gas (Fig. 8), it would be easy to maintain a high reaction temperature. Thus, catalytic activity at the lower temperature is not necessary, and Cu/Al_2O_3, which exhibits catalytic activity at a higher temperature, can be used. If the temperature rises beyond 1073 K, NO_x would be generated due to thermal decomposition,[7] and at the same time thermal sintering would probably be accelerated. Therefore, controlling the temperature by such means as dilution of the ingredients and multi-feeding of ingredients for equalizing the temperature in the catalyst bed is necessary in an actual plant.

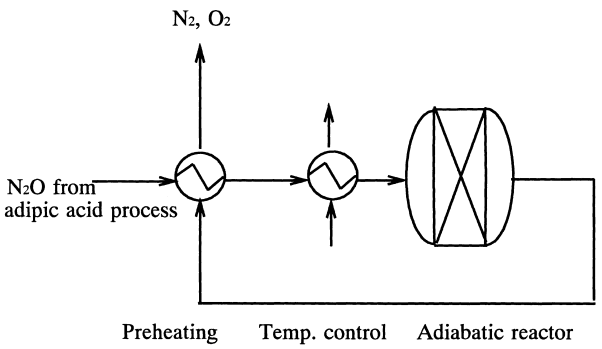

Fig. 8. Catalytic decomposition process for N_2O abatement.

Conclusion

We summarize the results as follows: (1) The activation energy is estimated to be 113 kJ/mol for a N_2O decomposition reaction with Cu/Al_2O_3 containing 3 wt% of Cu. (2) The apparent activation energy is estimated to be 167 kJ mol^{-1} in the lower temperature range (746 to 853 K). The difference in the activation energy is explained in terms of the inhibition effect of oxygen adsorbed on the surface of the catalyst; the adsorption equilibrium constants is estimated to be K_{O_2} = 28.9–2.8 atm^{-1} between 746 and 813 K. (3) The reaction rate constant decreases with time. The decrease obeys a first-order equation with respect to the rate constant. The deactivation rate constant increases with the amount of N_2O reacted. Thermal sintering is a possible deactivation mechanism. (4) Simulation of the deactivation of the catalyst demonstrates that 15 m^3 of Cu/

Al_2O_3 is effective for 600 days for the treatment of N_2O generated from an adipic acid plant with a 12,000 t y^{-1} production capacity. It is presumed that the deactivation of the catalyst begins at the center of the catalyst bed and then proceeds through the rest of the catalyst bed. According to our calculations, the catalyst is deactivated almost homogeneously throughout the catalyst bed. The results of the simulation indicate that a Cu/Al_2O_3 catalyst can be used in industrial adipic acid plants for dinitrogen oxide abatement.

References

1 M. H. Thiemens and W. C. Trogler, *Science*, **251**, 932 (1991).

2 International Panel on Climate Change, "IPCC guide lines for national greenhouse gas inventories, chapter 4, Agriculture, Nitrous oxide from agricultural soils and manure management," OECD, Paris (1997).

3 R. F. Weiss, *J. Geophys. Res., C: Oceans Atomos.*, **86**, 7185 (1981).

4 M. A. K. Khalil and R. A. Rasmussen, *Tellus, Ser. B*, **35**, 161 (1983).

5 A. Shimizu, K. Tanaka, and M. Fujimori, *Chemosphere Global Change Sci.*, **2**, 425 (2000).

6 R. A. Reimer, C. S. Slaten, M. Seapan, T. A. Koch, and V. G. Triner, "Non-CO_2 Greenhouse Gases: Scientific Understanding, Control and Implementation" ed by J. van Ham et al., Kluwer Academic Publishers, Netherlands (2000), pp. 347–358.

7 R. A. Reimer, C. S. Slaten, M. Seapan, M. W. Lower, and P. Ez. Tomlinson, *Technologie Chimiche*, **6**, 81 (1995).

8 R. A. Reimer, C. S. Slaten, M. Seapan, M. W. Lower, and P. E. Tomlinson, *Environ. Prog.*, **13(2)**, 134 (1994).

9 Y. Li and J. N. Armor, *Appl. Catal., B*, **1**, L21 (1992).

10 F. Kapteijn, J. Rodriguez-Mirasol, and J. A. Moulijn, *Appl. Catal., B*, **9**, 25 (1996).

11 B. W. Riley and J. R. Richmond, *Catal. Today*, **17**, 277 (1993).

12 A. Dandekar and M. A. Vannice, *Appl. Catal., B*, **22**, 179 (1999).

13 O. Levenspiel, "Chemical Reaction Engineering," Sec. ed, John Wiley & Sons, New York (1972), pp. 537–562.

14 M. V. Twigg and M. S. Spencer, *Appl. Catal., A*, **212**, 161 (2001).

15 L. Rheaume and G. Parravano, *J. Phys. Chem.*, **63**, 264 (1959).

16 T. Yamashita and A. Vannice, *J. Catal.*, **161**, 254 (1996).